Thermal shockwaves in an upland river

PLEASE CITE THE PUBLISHED VERSION

http://dx.doi.org/10.1002/wea.2435

PUBLISHER

Wiley / © Royal Meteorological Society

VERSION

AM (Accepted Manuscript)

Thermal shockwaves in an upland river

Robert L. Wilby[1], Matthew F. Johnson[1] and Julia A. Toone[2]

[1] Department of Geography, Loughborough University, Loughborough, Leicestershire, LE11 3TU, UK

[2] Environment Agency, Trentside Office, Nottingham, NG2 5FA, UK

Accepted for publication: *Weather*

Date of acceptance: 11 August 2014

Corresponding author:

Robert L Wilby

Department of Geography

Loughborough University

Loughborough

Leicestershire

LE11 3TU, UK

Email: r.l.wilby@lboro.ac.uk

Tel: +44 1509 223093

Abstract

We investigate the genesis and propagation of thermal 'shockwaves' using one of the densest arrays of paired air-water thermistors in the UK. Three onset mechanisms were detected in the River Dove driven by: solar radiation under stable flow and clear skies; rapid cooling by snowmelt; or runoff from intense summer rainfall. Largest absolute temperature changes were solar driven, but greatest rates of change (+3 degC in 15 minutes) were triggered by summer storms. These shockwaves travel downstream at lower velocities than hydropeaks. Climate models project more extreme rainfall so thermopeaks could exert greater influence on freshwater taxa in the future.

Key words: Water temperature; solar radiation; summer rainstorm; thermopeak; River Dove

Introduction

River temperature (Tw) is a fundamental determinant of water quality, chemical rates, biological processes, and organism behaviour (Webb et al., 2008). As such, there is concern that rising Tw and changing patterns of river flow under anthropogenic climate change could adversely impact freshwaters (Caissie, 2006; Orr et al., 2014). Hence, there are calls for active management of surface/groundwater flows and riparian vegetation to safeguard cool refugia and vulnerable species (Hansen et al., 2003). At the same time it is recognised that such interventions should be founded on process-understanding obtained through field observation and modelling (Wilby et al., 2010).

Field studies of the energy fluxes controlling Tw show that approximately 70% of heat input originates from solar radiation, with the remainder provided mainly by friction of water with the river bed and banks, and sensible heat transfer from the atmosphere (Webb et al., 2008). Air temperature (Ta) is widely used as a surrogate for solar radiation in empirical models for predicting Tw variations over time-scales of days to months (Johnson et al., 2014). The most significant heat outputs are radiation, evaporation, bed conduction and sensible heat transfer across the water-air interface. Local factors such as landscape shading, river orientation and vegetation cover affect receipts of solar radiation; groundwater fed streams may have increased longwave, latent and sensible heat losses (in winter); channel morphology, river flow and artificial structures influence heat advection from upstream. Global mean annual Tw is approximately 14 degC but there are large regional variations. Maximum Tw can reach 35 degC in equatorial, arid and warm temperate climate zones, however, mean Tw varies between 4 degC and 27 degC in polar and equatorial regions respectively (Punzet et al., 2012).

We deploy a high resolution thermistor array to investigate rapid Tw variations linked to weather conditions. We favour these instruments because of their low cost and accuracy which enable detailed sampling of Tw in space and time. Alternatives such as airborne remote sensing can yield high quality information on spatial patterns of surface Tw but only for snapshots in time and where the river is not obscured (Torgersen et al., 2001). Conversely, site-specific monitoring of heat budget components provides detail on temporal variations in Tw but is less feasible for large numbers of locations (Webb et al., 2008). Fibre optic methods offer high spatial and temporal resolution but only over distances of up to several kilometres (Krause et al., 2013).

Here, we focus on acute as opposed to chronic Tw changes because of their potential for sudden onset and significant ecosystem impacts (Beaulieu et al., 2013; Bruno et al., 2013; McHenry and Long, 1995). Rapid Tw increases (thermopeaks) have been reported under a range of artificial conditions including thermal discharges from power stations (Langford and Aston, 1972); warm water releases in winter (Dickson et al., 2012; Webb, 1995) and cool water in late spring/summer (Zolezzi et al., 2011) from hydropower reservoirs; as well as warm runoff from summer storms over paved surfaces (Herb et al., 2008; Sabouri et al., 2013).

Natural causes of rapid Tw reductions have also been documented. For example, Smith and Lavis (1975) describe decreases in Tw associated with individual rainfall and snowmelt events. Maybeck (2004) also recounts how a summer thunderstorm released sufficient cool water into the Pemigewasset River, New Hampshire for Tw to fall by 7 degC within six hours. Similarly, Gammons et al. (2005) note a modest Tw reduction associated with a hail storm in Butte Montana, US and Lange and Haensler (2012) observed significant drops in Tw when post-drought storm runoff was dominated by event water in the Black Forest, Germany.

Conversely, Langan et al. (2001) assert that the thermal impact of storm events is seasonally dependent and can yield Tw increases when heat is advected from riparian wetlands. Subehi et al. (2010) show the importance of hillslope gradient and water table depth in determining the hydrological pathway (i.e., relative mix of surface/sub-surface runoff) and hence Tw response to rainfall in small forested catchments. Brown and Hannah (2007) found that short-duration low-intensity storms falling onto an alpine catchment can occasionally produce Tw increases of up to 2.3 degC.

From the above synopsis it is evident that meteorological controls of river temperature responses are mediated by antecedent river flow and catchment conditions (such as soil temperature and moisture content), type of land cover, topography, contributions from groundwater, attributes of the generating event, and so forth. The purpose of this study is to use a high-resolution thermistor array to 1) establish a typology of rapid, sub-daily Tw changes; and 2) present empirical evidence of the magnitude of Tw change, rate of downstream propagation and dispersion of these short-lived phenomena. The ultimate aim of the research is to improve understanding of the drivers and raise awareness of the potential significance of thermal 'shockwaves' for temperate river ecosystems.

Study area, data and methods

The study catchment and field experiments are described by Wilby et al. (2012), Johnson et al. (2014) and online at http://www.luten.org.uk. The Loughborough University TEmperature Network (LUTEN) comprises 36 sites with synchronised Tw and Ta measurements in the rivers Dove and Manifold of the English Peak District (Figure 1). Pasture is the main land-use in both catchments and elevations range from 150 to 450 m. This study employs a sub-set of the data collected in the Dove catchment (sites D1 to D23) which is fed largely by groundwater seepage plus flows from non-thermal and semi-thermal springs along the margin of the Limestone outcrop (Edmunds, 1971). These sources discharge at relatively constant temperatures year-round thereby lowering ambient Tw in summer but increasing Tw in winter (Johnson *et al.*, 2014). Parts of the headwaters and lowest reaches of the Dove are in deep landscape shade, whereas middle sections are most exposed to direct solar radiation.

Two Gemini *Tinytag* Aquatic 2 thermistors record maximum, mean and minimum temperatures every 15-minutes at each site: one on the river bed measuring Tw; the other at about 2 m above the water surface measuring Ta. Tinytag sensors have a quoted accuracy of 0.2 degC which we checked under field and laboratory conditions (Johnson and Wilby, 2013). To avoid heating by direct solar radiation sensors were fixed in deep shade. Data reported here are for three years March 2011 to February 2014.

Fifteen-minute river flow data were acquired from two gauges kept by the Environment Agency (EA). The Hollinsclough (HC) gauge is in the upper Dove and has a drainage area of 8 km^2; the Izaak Walton (IW) gauge is downstream and represents a catchment of 83 km^2 (Figure 1). According to the National River Flow Archive both river flow records are defined as ‘natural to within 10% at the 95th percentile’ (although for HC river flow estimates >0.8 m^3s^{-1} are based on rating tables and should be treated with caution). Note also that there are more than 100 shallow weirs and occasional sub-surface field drains in the lower reaches of the Dove (between D17 and D24).

Daily precipitation totals were acquired from UK Met Office stations at Buxton (53°15’N, 1°55’ W) and Ashbourne (53°1’N, 1°44’ W). These lie ~10 km to the north of the source and south of Dovedale (D24) respectively. Hourly precipitation data were obtained from stations at Coton-in-the-Elms (52°44’N, 1°38’ W), Keele (53°0’N, 2°16’ W), Leek (53°8’N, 1°59’ W) and Hollinsclough (53°12’N, 1°54’ W) within the headwaters of the Dove.

We objectively identified thermopeaks using the rate of change (ROC) of Tw over one hour at site D10 (Figure 1). We did not discriminate between rising or falling limbs but only take note of the most extreme value (whether positive or negative) each day. We then ranked all days and extracted the 12 largest absolute ROC along with antecedent precipitation total, air temperature (at D10) and concurrent river flow in each case. Site D10 was chosen because of its central location within the catchment (above the Limestone gorge) and because the record is 97% complete. Moreover, the Tw series at D10 is most highly correlated (average r=0.98) with all other sites in the Dove, so is regarded to be representative.

Finally, we estimate thermal and flood (or hydrodynamic) wave velocities with the expectation that they are asynchronous. This is because the thermal peak behaves as a passive tracer and is advected downstream at the velocity of water molecules depending on river flow depth and channel roughness. This advective heat transport is further influenced by local heat exchange with the stream bed, hyporheic exchange or storage within in-stream 'dead-zones' (Evans et al. 1998, Neilson et al. 2010, Westhoff et al. 2010; 2011). Meanwhile, the flood wave travels more quickly than water molecules with the velocity depending on free surface width, volume and depth of flow relative to pre-event conditions (Toffolon et al., 2010).

If the thermal wave was triggered by a storm, event initiation was assumed to be the time of peak rainfall intensity measured at Hollinsclough (the closest gauge). Downstream variations in thermal wave velocity were then determined using distance between sites and time of arrival of peak Tw. Velocities for hydrodynamic waves were estimated using the known distance between HC and IW (27.9 km) and the difference in time of arrival of the hydrograph peak at each gauge to the nearest 15 minutes.

Results

Our three year monitoring period included several notable hydrological events. For example, spring 2011 had the most severe and widespread April snow storm since 1981. Violent storms in late June and early July 2012 brought flash flooding across numerous locations in England and Wales (Almond, 2013; Clark and Webb, 2013). These episodes also contributed to the wettest April to July in nearly 250 years and brought an abrupt end to one of the most significant prolonged droughts in a century (Kendon et al., 2013; Parry et al., 2013). The first week of May 2013 was notable for the amount of bright sunshine which reached 14 hours on some days. Winter 2013/14 was confirmed as the wettest since 1766 in the England and Wales precipitation series, with more than 130% average rainfall locally in the Peak District (Met Office, 2014).

Figure 2 shows the ROC trace for site D10 in 2012/13. This series is strongly correlated (r=0.9) with ROC data up and downstream (sites D6 and D16 respectively). ROC values seldom exceed ±1 degC/hour so events with rapid Tw change clearly stand out (as in the case of 4 April 2012, 28 June 2012, 5 July 2012 and 27 January 2013). Across the three years of data, the 12 largest ROC scores all exceeded ±0.8 degC/hour at D10 (Table 1). Overall, the most extreme ROC (15 minute) for any site was +3 degC recorded at site D1 between 2030 UTC and 2045 UTC on 5 July 2012.

Three types of event were distinguished by inspection of the full data set (Table 1). Overall, the most rapid positive Tw changes were preceded by intense rainfall (*IR*); the two most extreme negative ROCs were linked to heavy snowfall and/or melt (*SM*). The remaining events occurred on days with zero precipitation, stable or falling river flow, and large diel Ta ranges (typically > 17 degC). These events were all preceded by nocturnal cooling then by intense solar heating (*SH*) under clear sky conditions. The most extreme ROC (per hour) at D10 for each category of event was +2.8 degC for *IR*, -1.3 degC for *SM*, and +1.2 degC for *SH* (Table 1).

Figure 3 shows examples of the downstream propagation of thermal waves generated by these three mechanisms. Under intense *SH* events, Tw increases most rapidly between mid-morning and mid-afternoon at upstream sites. The thermal wave is modified by heat exchanges between atmosphere and river as it advects downstream, typically arriving at sites above the spring line (D16) between 1700 UTC and 2000 UTC (Figure 3a). The magnitude of the diel Tw range depends on the volume of flow (i.e., thermal inertia of the water body), strength of solar shortwave radiation, net longwave radiation, convection, and evaporation heat fluxes (Evans et al., 1998). The damped response of Tw between D16 and D23 shows that groundwater inputs reduce the diel range even when there is strong radiant forcing upstream.

Under *SM* events (such as 4 April 2012) relatively cold water enters the drainage network either directly as precipitation or indirectly as melt-water from ablating snow cover. The thermal sag drifts downstream such that absolute Tw minima experienced at downstream sites occur hours after detection in the headwaters (Figure 3b). Again, the markedly different Tw behaviour at D23 compared with upstream reflects the input of relatively warm groundwater. The thermal constancy of spring sources is evidenced by the similarity of the signal for D23 under *SH* and *SM* forcing (Figures 3a and 3b).

The most dramatic thermal response occurs after *IR* events (Figures 3c and 3d). The exact shape of the thermopeak depends on the attributes of the generating storm (duration, maximum intensity, and direction of travel relative to the main channel orientation). The thermal wave on 28 June 2012 (Figure 3c) was initiated by an intense storm with maximum precipitation rate >13 mm/hour at Hollinsclough (Figure 4a). The hydrograph response at the upstream gauge was subdued compared with downstream reflecting the SW to NE passage of the frontal system and zone of maximum rainfall intensity which was located to the south.

The peak rainfall intensity on 5-6 July 2012 was lower (~9 mm/hour) than on 28 June 2012 (Figure 4a and 4b) but a greater total fell onto ground that was already saturated (as indicated by the higher initial river flows in Table 1). Storm onset was marked by a rapid drop in Ta and near immediate rise in river flow at the HC gauge (Figure 3d). Coincident thermal peaks at D1 and D16 may indicate earlier arrival of a local rainstorm at the downstream site. An alternative explanation is that runoff from paved surfaces in the hamlet of Mill Dale added warm water to the river between D16 and D20. The spring site (D23) exhibited a damped but earlier than expected thermal response to both *IR* events. This was attributed to a sub-surface field drain that discharges from the west-facing escarpment into the river between sites D22 and D23.

Consistent with theory, hydrodynamic wave velocities were higher than thermal wave velocities as indicated by shorter travel times to fixed sites (Figure 5). Non-linear time-distance relationships show that the thermal wave is decelerating. The most rapid hydrodynamic wave followed high intensity rainfall over the whole catchment (28 June 2012) whereas the most rapid thermal wave trailed lower intensity rainfall but relatively high totals in the headwaters (5-6 July 2012). Hence, depending on the spatial-temporal dynamics of the storm, the estimated travel time of the hydrodynamic wave between HC and IW varied between 270 and 435 minutes (equivalent to 1.1 - 1.7 ms^{-1}) compared with 619 to 951 minutes (or 0.5 - 0.8 ms^{-1}) for the thermal wave.

The travel time analysis indicates that following *IR* events stream biota are exposed first to rising river flow then second to a thermal shock. The separation time between the two waves increases with distance from source. Under the most extreme case (28 June 2012) the estimated time interval between arrival of the hydrodynamic and thermal waves at IW was >11 hours. Furthermore, at sites above the spring zone, the duration of the event (as indicated by the time for Tw to return to pre-event values) increases downstream due to turbulent diffusion and shear flow dispersion. For example, the thermal wave on 28 June 2012 increased Tw for 645 minutes at site D1 and 855 minutes at D10.

The following section considers the wider implications of these findings including the potential significance of thermal waves for freshwater taxa.

Discussion

Based on data from LUTEN we have detected three mechanisms that can generate rapid responses in river temperatures. These are heating by solar radiation under clear skies and low flow conditions; cooling by direct snowfall and/or melt-water runoff; or heating by runoff produced by intense summer storms. Heating by solar radiation typically yields maximum Tw at downstream sites just after sunset (Figure 3a). However, a noteworthy feature of *IR* events is that abrupt changes and maximum Tw can occur during the night, at times when Tw would otherwise be dominated by net radiant losses (Evans et al., 1998).

Moreover, *IR* events generate the most rapid sub-daily Tw changes: up to +3 degC in 15 minutes for the most extreme case (D1 on 5 July 2012).

These observations arise from a small sample of events that were identified objectively via ROC values. In general, *IR* events are expected to be most severe when Ta > Tw, there has been strong solar heating of the land surface, the storm is intense, and initial river flow is low (Herb et al., 2008). The three most extreme *IR* events all occurred during a two week period of remarkable transition from drought to flooding (Parry et al., 2013). However, additional thermal waves emerge when the ROC threshold is relaxed to a threshold of ±0.5 degC/hour. For example, following >60 mm rainfall at Buxton on 27 July 2013, a ROC of +0.6 degC/hour was recorded. Another event on 18 July 2011 was triggered by >65 mm rainfall at Leek which led to an abrupt increase in river flow and was marked by the arrival of warmer water from upstream of D23. This diluted the signature of cooler spring water and caused Tw to change +1.6 degC between 0400 UTC and 0415 UTC at D23 (Figure 6).

Primary and secondary *IR* events in the Dove are generally associated with daily rainfall totals >20 mm at Buxton. Analysis of records since year 1961 suggests that rainfall totals of this magnitude or more occur between zero to four times per summer (June to August). However, variations in the features of individual thermal waves are explained by several other factors operating in the Dove.

First, abrupt heating or cooling is superimposed on diel and annual Tw regimes which are governed by seasonal variations in solar heating and river flow (Webb and Walling, 1985). Second, thermal wave propagation and longitudinal dispersion are affected by the extent of pre-heating and ponding behind the weirs between D16 and D23. Third, absence of tributaries limit scope for mixing of thermally contrasting water in the upper Dove, but this is not the case where field drains and springs feed into the lower reaches. Evidence of distinct thermopeaks in the main stem of the dendritic network of the river Manifold (not shown) implies that the influence of surface runoff from tributaries may not be significant in these small catchments.

We venture that *IR* events may be generating thermal waves in other natural headwaters in the UK. For the Dove, the thermal wave amplitude was greatest ~10 km from source, dissipating thereafter even before encountering cooler groundwater. Hence, we speculate that catchments with areas <100 km^2 and flashy hydrological regimes might be particularly vulnerable (but scope for testing this hypothesis elsewhere is constrained by data availability).

Other factors such as channel gradient, roughness, pool-riffle sequencing, connectivity to floodplain, and artificial structures influence the local velocity of the thermal wave and thereby space-time variations in heat budget. Land cover and soil moisture conditions determine the fraction of solar energy partitioned into sensible heating of the surface prior to storm onset. For instance, streams draining urbanised catchments are known to exhibit thermo-peaking after strong solar heating and heavy rainfall (Herb et al., 2008; Sabouri et al., 2013). Conversely, larger catchments have greater scope for turbulent diffusion and shear flow dispersion with distance downstream. There may also be tributaries and groundwater units which mix thermally contrasting water into the main channel flow.

Abrupt changes in Tw are known to trigger a range of sub-lethal, biological responses. For example, benthic invertebrates exhibit species- and season-dependent avoidance strategies under carefully controlled laboratory conditions (Carolli et al., 2012). Moreover, because of synergistic effects, asynchronous hydro- and thermo-peaks cause greater density of invertebrate movement than hydro- or thermo-peaks alone (Bruno et al., 2013). Due to increasing separation time between the two peaks with distance downstream a spatial signature in invertebrate response is expected. Tw is also an important behavioural cue for the timing of feeding in juvenile Atlantic salmon (*Salmo salar*) which occurs preferentially at night when Tw falls below 10 degC (Fraser et al. 1993). Hence, arrival of a thermal wave during hours of darkness may be particularly significant for nocturnal creatures (Wilby et al., 2014).

Climate model projections show increased likelihood of extreme rainfall linked to higher atmospheric temperatures and vapour content (Trenberth, 2011). On the other hand, a scenario of higher Ta implies that the frequency of snowfall in the UK could diminish. Under these conditions, occurrence of *IR* events would be expected to increase, whereas *SM* events could become rarer. However, the future magnitude and frequency of thermal waves also depends on the antecendent conditions of the receiving water course. Climate model outlooks for the UK are ambiguous for winter, but there is greater consensus that river flows could decrease in summer (Prudhomme et al., 2012). A hotter, drier summer climate, with lower flow volumes, would pre-dispose rivers to more frequent *SH* and *IR* events. One high resolution (1.5 km) climate model experiment suggests that the frequency of very heavy rainfall episodes in summer could nearly quadruple by 2100 (Kendon et al., 2014).

Conclusions

We have evidence of the genesis and propagation of thermal waves in a ‘natural’ headwater river. Three onset conditions were identified: bright sunshine, heavy snowfall/melt, or intense summer rainfall. These phenomena matter because they potentially affect water quality and produce sub-lethal behavioural responses in biota. Our results also demonstrate that thermal waves can occur under meteorological conditions other than strong solar radiation. One implication of this finding is that increased riparian shade is not a complete panacea for warming rivers because it would afford little protection against storm generated Tw changes.

Further research is needed to determine whether abrupt Tw increases are occurring in other catchments and the extent to which these phenomena are mediated by regional climate and land surface properties. It is also unclear which taxa might be most sensitive to thermal waves and the extent to which any trends in timing, magnitude and frequency of these events might be detectable as changes in ecosystem structure and function. Some have begun to explore such questions under laboratory conditions to mimic thermo-peaking below dams, but this work is largely restricted to invertebrate behaviour. Whereas conventional (monthly, day-time) spot-sampling of Tw may be barely sufficient for tracking environmental change over decadal time-scales, this is clearly insufficient for discerning biologically relevant thermal cues at storm-event scales.

Acknowledgements

The authors thank the landowners who kindly granted access to the field sites, the Met Office for providing meteorological data, as well as the Wild Trout Trust and Trent Rivers Trust for supporting the purchase of equipment. Data from the LUTEN network may be obtained from: http://www.luten.org.uk/ or by contacting the authors.

References

Almond C. 2013. Heavy rain and flooding in southwest England on 6-7 July 2012. *Weather*, **68**: 171-175.

Beaulieu JJ, Arango CP, Balz DA, Shuster WD. 2013. Continuous monitoring reveals multiple controls on ecosystem metabolism in a suburban stream. *Freshwater Biology*, **58**: 918-937.

Brown LE, Hannah DM. 2007. Alpine stream temperature response to storm events. *Journal of Hydrometeorology*, **8**: 952-967

Bruno MC, Siviglia A, Carolli M, Maiolini, B. 2013. Multiple drift responses of benthic invertebrates to interacting hydropeaking and thermopeaking waves. *Ecohydrology*, **6**: 511-522.

Caissie D. 2006. The thermal regime of rivers: a review. *Freshwater Biology* **51**: 1389–1406.

Carolli M, Bruno MC, Siviglia A, Maiolini B. 2012. Responses of benthic invertebrates to abrupt changes of temperature in flume simulations. *River Research and Applications* **28**: 678-691.

Clark MR, Webb JDC. 2013. A severe hailstorm across the English Midlands on 28 June 2012. *Weather*, **68**: 284-291.

Dickson NE, Carrivick JL, Brown LE. 2012. Flow regulation alters alpine river thermal regimes. *Journal of Hydrology*, **464**: 505-516.

Edmunds WM. 1971. *Hydrogeochemistry of groundwaters in the Derbyshire Dome with special reference to trace constituents*. Report of the Institute of Geological Sciences, 71/7, British Geological Survey, Keyworth.

Evans EC, McGregor G, Petts GE. 1998. River energy budgets with special reference to river bed processes. *Hydrological Processes* **12**: 575–595.

Fraser NHC, Metcalfe NB, Thorpe JE. 1993. Temperature-dependent switch between diurnal and nocturnal foraging in Salmon. *Proceedings of the Royal Society of London B* **252**: 135–139.

Gammons CG, Shope CL, Duaime TE. 2005. A 24 h investigation of the hydrochemistry of baseflow and stormwater in an urban area impacted by mining: Butte, Montana. *Hydrological Processes*, **19**: 2737-2753.

Hansen LJ, Biringer JL, Hoffman JR (eds.) 2003. *Buying time: a user's manual for building resistance and resilience to climate change in natural systems*. WWF Climate Change Program, Berlin, Germany, 244pp.

Herb WR, Janke B, Mohseni O, Stefan HG. 2008. Thermal pollution of streams by runoff from paved surfaces. *Hydrological Processes*, **22**: 987-999.

Johnson MF, Wilby RL. 2013. Shield or not to shield: Effects of solar radiation on water temperature sensor accuracy. *Water* **5**: 1622–1637.

Johnson MF, Wilby RL, Toone JA. 2014. Inferring air-water temperature relationships from river and catchment properties. *Hydrological Processes*, **28**: 2912-2928.

Kendon EJ, Roberts NM, Fowler HJ, Roberts MJ, Chan SC, Senior CA. 2014. Heavier summer downpours with climate change revealed by weather forecast resolution model. *Nature Climate Change*, **doi**: 10.1038/NCLIMATE2258.

Kendon M, Marsh T, Parry S. 2013. The 2010-2012 drought in England and Wales. *Weather*, **68**: 88-95.

Krause S, Taylor SL, Weatherill J, Haffenden A, Levy A, Cassidy NJ, Thomas PA. 2013. Fibre-optic distributed temperature sensing for characterizing the impacts of vegetation coverage on thermal patterns in woodlands. *Ecohydrology*, **6**: 754-764.

Langan SJ, Johnston L, Donaghy MJ, Youngson AF, Hay DW, Soulsby C. 2001. Variation in river water temperatures in an upland stream over a 30- year period. *Science of the Total Environment*, **265**: 195-2007.

Lange J, Haensler A. 2012. Runoff generation following a prolonged dry period. *Journal of Hydrology*, **464**: 157-164.

Langford TE, Aston RJ. 1972. The ecology of some British rivers in relation to warm water discharges from power stations. *Proceedings of the Royal Society London B*, **180**: 407-419.

Maybeck HF. 2004. *Rapid river water temperature fluctuations*. U.S. Geological Survey, Natural Streamflow Information Program. River Gage Station USGS #01076500 Pemigewasset River at Plymouth, New Hampshire, US.

McHenry MJ, Long JH Jr. 1995. A rapid increase in water temperature alters the swimming performance of striped bass (*Morone saxatilis*). In: Blair, E.A. and Waldman, J.R. (eds.). *Final Reports of the Tibor T. Polgar-Fellowship Program*, Section V, pp1-18. Hudson River Foundation, New York, US.

Met Office. 2014. UK seasonal weather summary: winter 2013/2014. *Weather*, **69**: 99.

Neilson BT, Chapra SC, Stevens DK, Bandaragoda C. 2010. Two-zone transient storage modeling using temperature and solute data with multiobjective calibration: 1. Temperature. *Water Resources Research*, **46**: W12520.

Orr HG, Simpson GL, des Clers S, Watts G, Hughes M, Hannaford J, Dunbar MJ, Laize CLR, Wilby RL, Battarbee RW, Evans R. 2014. Detecting changing river temperatures in England and Wales. *Hydrological Processes*, doi:10.1002/hyp.10181.

Parry S, Marsh T, Kendon M. 2013. 2012: from drought to floods in England and Wales. *Weather*, **68**: 268-274.

Prudhomme C, Young A, Watts G, Haxton T, Crook S, Williamson J, Davies H, Dadson S, Allen S. 2012. The drying up of Britain? A national estimate of changes in seasonal river flows from 11 Regional Climate Model simulations. *Hydrological Processes*, **26**: 1115-1118.

Punzet M, Voβ F, Voβ A, Teichert E, Bärlund I. 2012. A global approach to assess the potential impact of climate change on stream water temperatures and related in-stream first order decay rates. *Journal of Hydrometeorology*, **13**: 1052-1065.

Sabouri F, Gharabaghi B, Mahboubi AA, McBean EE. 2013. Impervious surfaces and sewer pipe effects on stormwater runoff temperature. *Journal of Hydrology*, **502**: 10-17.

Smith K, Lavis ME. 1975. Environmental influences on the temperature of a small upland stream. *Oikos*, **26**: 228-236.

Subei L, Fukushima T, Onda Y, Mizugaki S, Gomi T, Kosugi K, Hiramatsu S, Kitahara H, Kuraji K, Terajima T. 2010. Analysis of stream water temperature changes during rainfall events in forested watersheds. *Limnology*, **11**: 115-124.

Toffolon M, Siviglia A, Zolezzi G. 2010. Thermal wave dynamics in rivers affected by hydropeaking. *Water Resources Research*, **W08536**.

Torgersen CE, Faux RN, McIntosh BA, Poage NJ, Norton DJ. 2001. Airborne thermal remote sensing for water temperature assessment in rivers and streams. *Remote Sensing of Environment*, **76**: 386-398.

Trenberth KE. 2011. Changes in precipitation with climate change. *Climate Research*, **47**: 123-138.

Webb BW. 1995. Regulation and thermal regime in a Devon river system. In: Foster, I.D.L., Gurnell, A.M. and Webb, B.W. (Eds) *Sediment and Water Quality in River Catchments*. John Wiley & Sons, Chichester.

Webb BW, Walling DE. 1985. Temporal variation of river water temperatures in a Devon river system. *Hydrological Sciences Journal* **30**: 449-464.

Webb BW, Hannah DM, Moore RD, Brown LE, Nobilis F. 2008. Recent advances in stream and river temperature research. *Hydrological Processes*, **22**: 902-918.

Westhoff MC, Bogaard TA, Savenije HHG. 2010. Quantifying the effect of in-stream rock clasts on the retardation of heat along a stream. *Advances in Water Resources*, **33**: 1417-1425.

Westhoff MC, Gooseff MN, Bogaard TA, Savenije HHG. 2011. Quantifying hyporheic exchange at high spatial resolution using natural temperature variations along a first order stream. *Water Resources Research*, **47**: W10508.

Wilby RL, Johnson MF, Toone JA. 2012. The Loughborough University TEmperature Network (LUTEN): Rationale and analysis of stream temperature variations. *Proceedings of Earth Systems Engineering 2012: Systems Engineering for Sustainable Adaptation to Global Change*. Newcastle, UK.

Wilby RL, Johnson MF, Toone JA. 2014. Nocturnal river water temperatures: Spatial and temporal controls. *Science of the Total Environment*, **482-483**: 157-173.

Wilby RL, Orr H, Watts G, Battarbee RW, Berry PM, Chadd R, Dugdale SJ, Dunbar MJ, Elliott JA, Extence C, Hannah DM, Holmes N, Johnson AC, Knights B, Milner NJ, Ormerod SJ, Solomon D, Timlett R, Whitehead PJ, Wood PJ. 2010. Evidence needed to manage freshwater ecosystems in a changing climate: turning adaptation principles into practice. *Science of the Total Environment*, **408**: 4150-4164.

Zolezzi G, Siviglia A, Toffolon M, Maiolini B. 2011. Thermopeaking in Alpine streams: event characterization and time scales. *Ecohydrology*, **4**: 564-576.

Table 1 Properties of 12 events with most rapid changes in Tw at site D10 between March 2011 and February 2014

Variable	**Sites**	**1/5/11**	**4/5/11**	**4/4/12**	**6/5/12**	**28/6/12**	**5-6/7/12**	**10/7/12**	**27/1/13**	**1/5/13**	**2/5/13**	**6/5/13**	**7/5/13**
P_{tot} (mm)	Buxton	0	0	8.4	0	4.7	11.7	17.3	0	0	0	0	0
P_{tot} (mm)	HC	0	0	18.8	0	17.2	30.6	13.6	6.6	0	0	0	0
P_{tot} (mm)	Ashbourne	0	0	11.4	0	16.8	18.2	5.4	0.6	0	0	0	0
Q_0 (m^3/s)	HC	0.071	0.070	0.093	0.178	0.278	0.351	0.330	0.958†	0.079	0.076	0.072	0.069
Q_0 (m^3/s)	IW	0.767	0.752	0.979	2.040	2.780	3.080	3.280	2.260	1.150	1.140	1.080	1.060
ΔQ (m^3/s)	HC	-0.001	-0.001	+0.028	0	+0.205	+11.35†	+5.09†	+2.63†	0	-0.002	-0.003	-0.001
ΔQ (m^3/s)	IW	-0.007	0	+0.421	0	+1.980	+7.12	+3.23	+9.44	-0.010	-0.020	-0.030	-0.020
Ta range (°C)	D10	11.3	18.3	2.4	17.6	11.1	14.0	4.5	5.3	17.5	19.7	22.2	20.2
Max ΔTw (°C/hr)	D10	+1.0	+1.0	-1.0	+0.9	+2.8	+2.4	+1.2	-1.3	+1.1	+1.1	+1.1	+1.2
ROC rank	D10	10	9	11	12	1	2	4	3	7	6	8	5
Max ΔTw (°C/hr)	(various)	+1.9 (D20)	+2.0 (D20)	-1.1 (D6)	+1.0 (D6)	+3.2 (D11)	+2.4 (D10)	+1.6 (D1)	-1.3 (D10)	+1.5 (D6)*	+1.2 (D6)*	+1.2 (D6)*	+1.3 (D6)*
	D23	+0.8	+0.8	-0.5	+0.8	+2.0	+1.2	+0.9	-0.8	+0.7	+0.7	+0.7	+0.7
Event type	All	*SH*	*SH*	*SM*	*SH*	*IR*	*IR*	*IR*	*SM*	*SH*	*SH*	*SH*	*SH*

Key: P_{tot} (precipitation total); Q_0 (pre-event discharge); ΔQ (change between pre-event and peak discharge); Ta range (diel air temperature range); Max ΔTw (maximum rate of change of water temperature per hour); ROC (rate of change); SH (solar heating); SM (snowmelt or snowfall); IR (intense rainfall); * D6 was the most upstream site after flood damage in summer/winter 2012/13; † Values outside the range used to calibrate the gauge.

Figure 1 LUTEN monitoring sites (red circles), EA gauging stations (black circles), Limestone outcrop (grey shading), sandstone and mudstones areas (unshaded). D10 is the reference site used to detect rapid changes in Tw across the network as a whole. Source: Wilby et al. (2014).

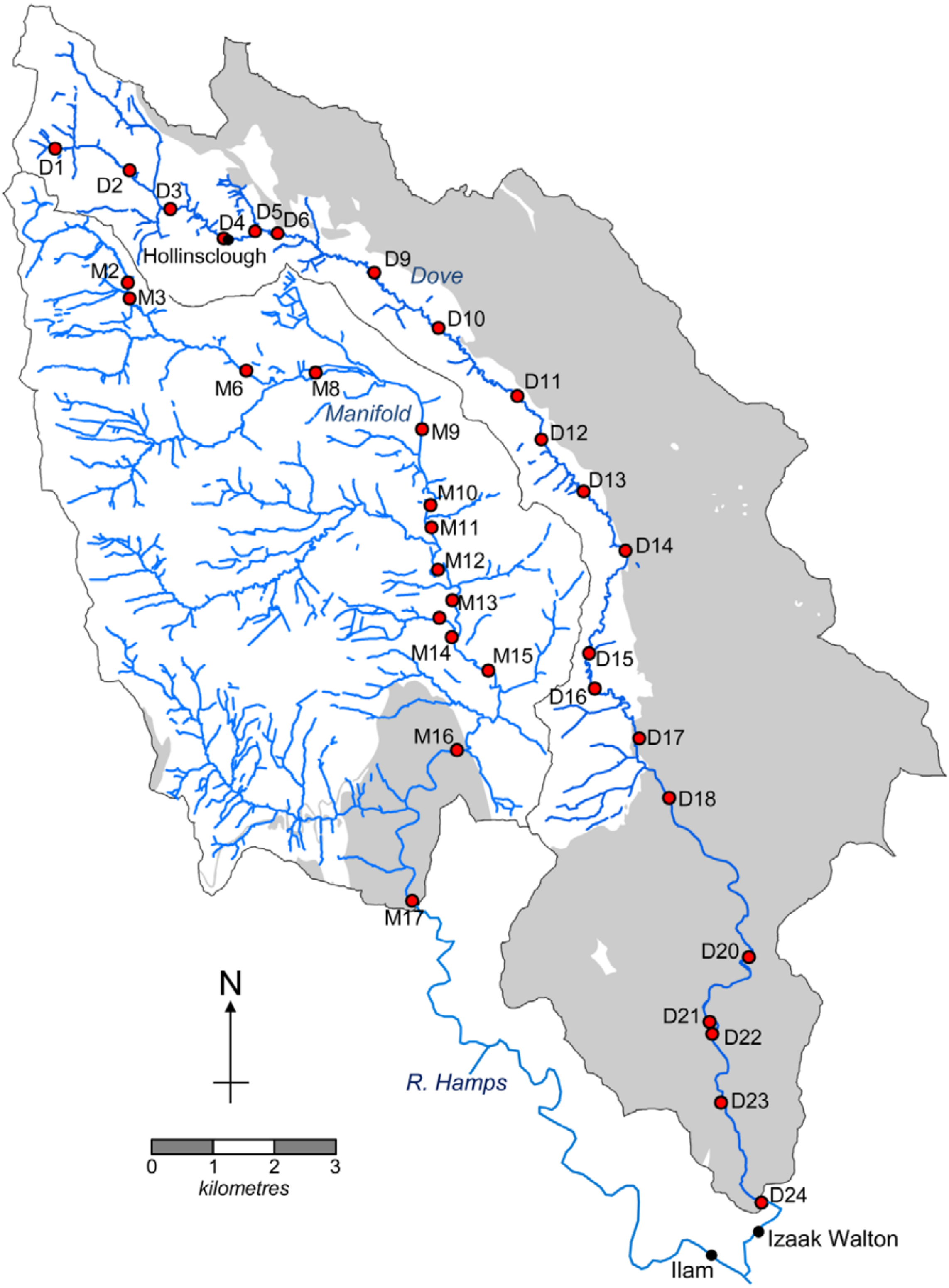

Figure 2 Example ROC series for site D10 during March 2012 to February 2013.

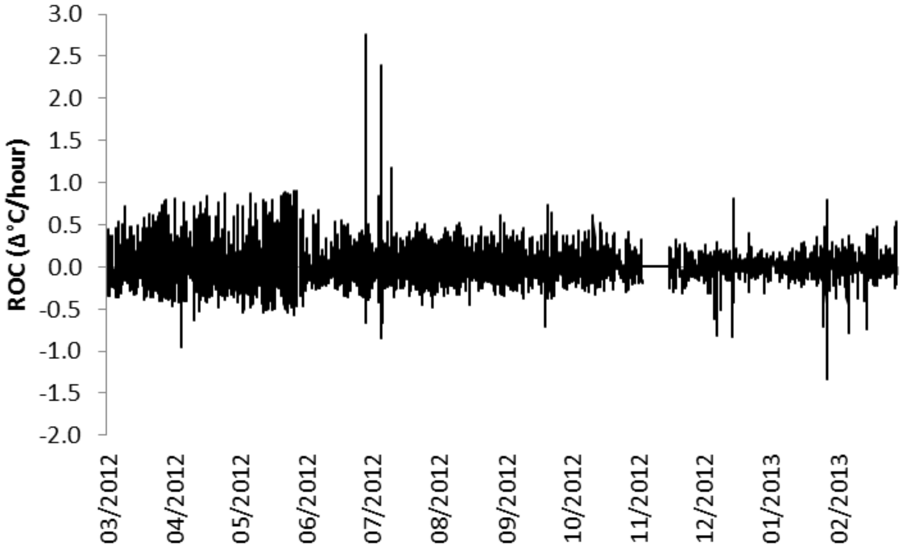

Figure 3 Example thermal waves produced by a) solar heating (4 May 2011), b) snow fall (4 April 2012), c) intense rainfall (28 June 2012) d) (5-6 July 2012). A 12 degC range is used for Tw, and 20 degC range for Ta. Accompanying hydrographs and air temperatures are also shown. The river flow gauges are Hollinsclough (HC) and Izaak Walton (IW).

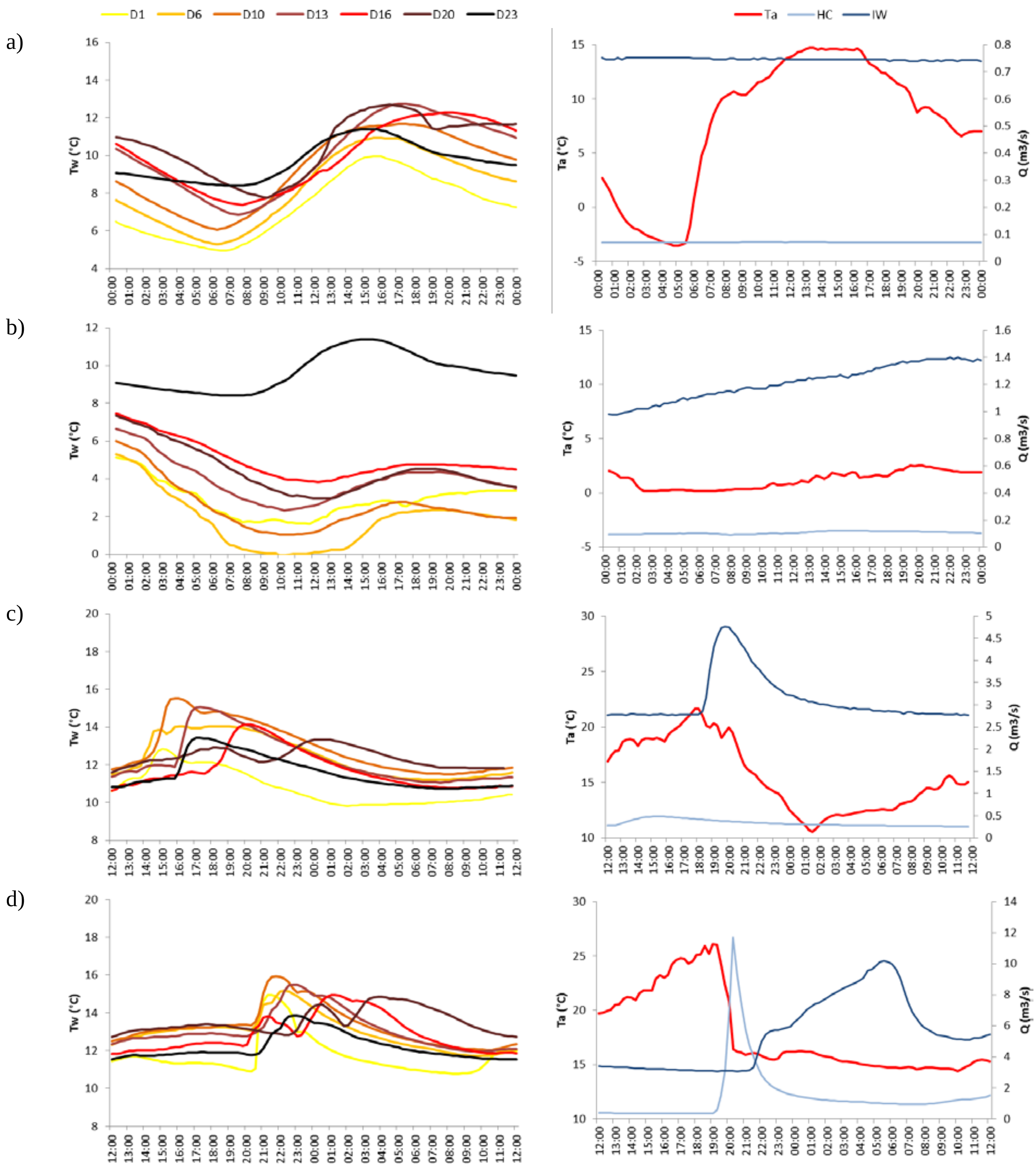

Figure 4 Hourly rainfall records associated with the three *IR* events shown in Table 1.

a) 28 June 2012

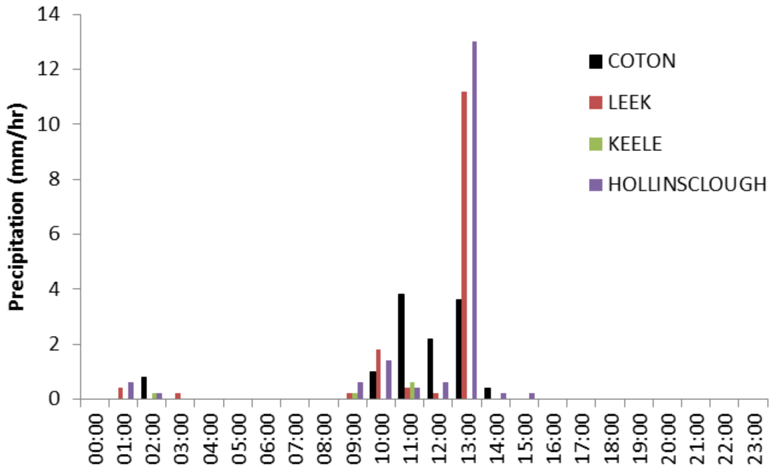

b) 5-6 July 2012

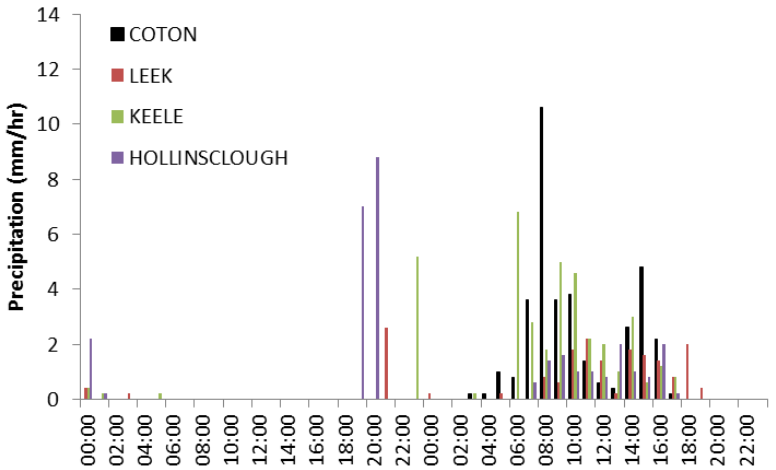

c) 10 July 2012

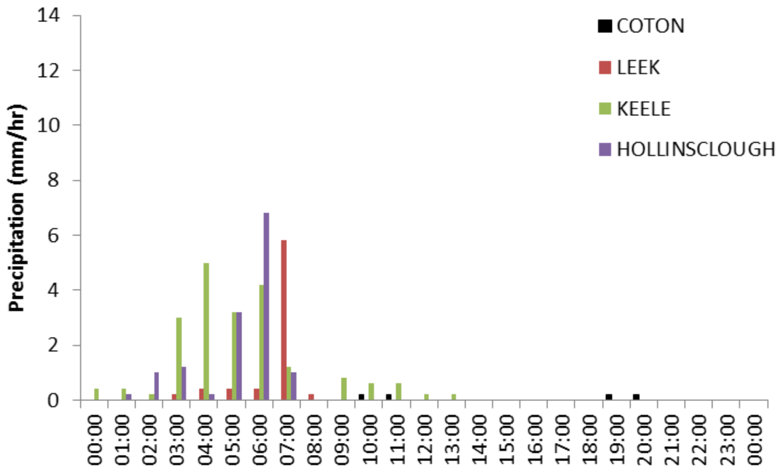

Figure 5 Times to thermo (**red** dots) and hydropeak (**blue** dots) following three intense rainfall (*IR*) events. Note that there are less data for July 2012 because sites D15 and D17 were washed out by high flows in the previous month.

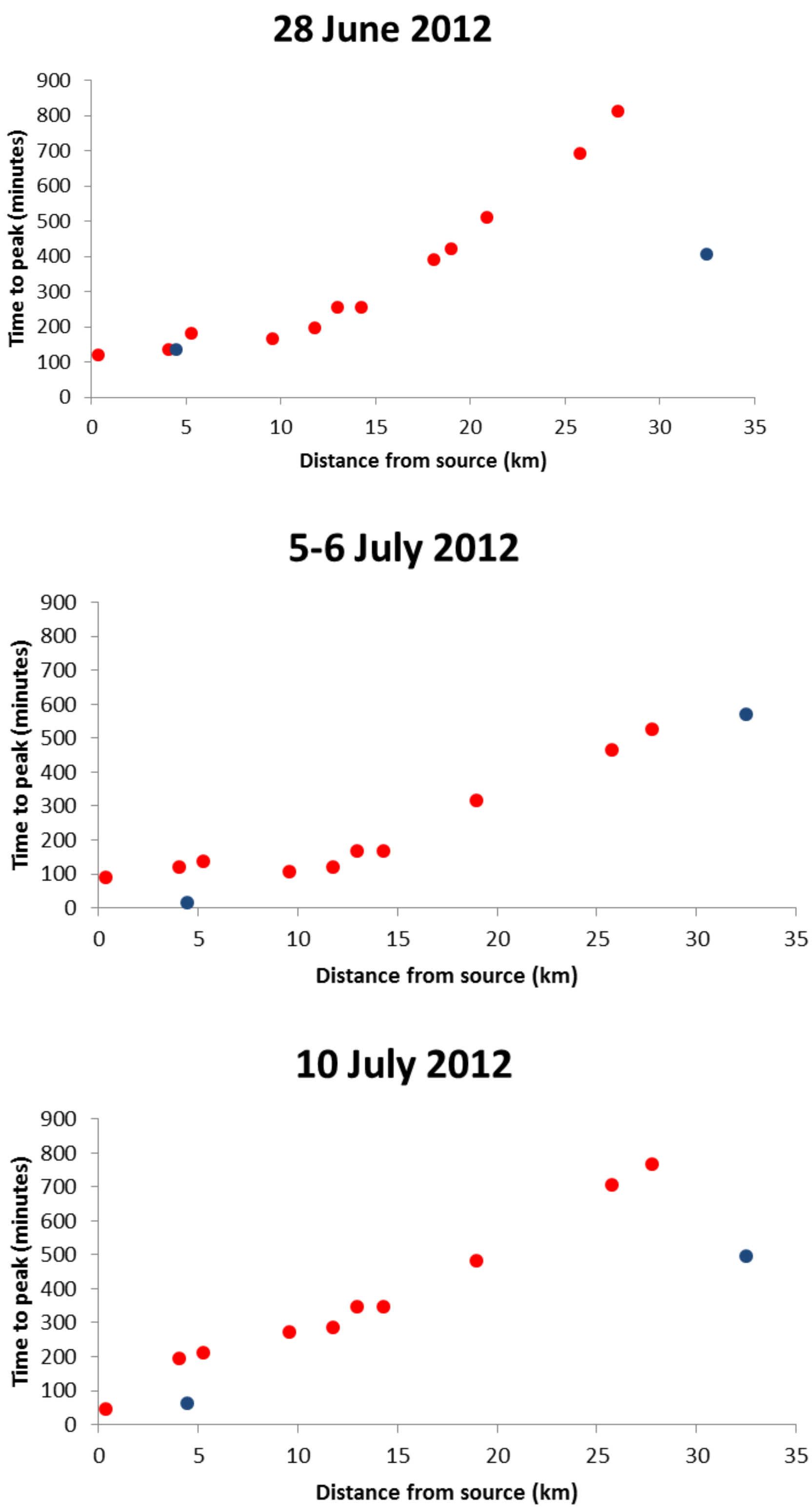

Figure 6 Detailed analysis of the *IR* thermal event of 17-19 July 2011